Available online at www.sciencedirect.com

ScienceDirect

Solar Energy 99 (2014) 67–76

SOLAR ENERGY

www.elsevier.com/locate/solener

Solar light induced photocatalytic degradation of Reactive Blue 220 (RB-220) dye with highly efficient Ag@TiO_2 core–shell nanoparticles: A comparison with UV photocatalysis

Ankita Khanna, Vidya K. Shetty *

Department of Chemical Engineering, National Institute of Technology Karnataka, Surathkal, Mangalore 575 025, India

Received 8 August 2013; received in revised form 22 October 2013; accepted 24 October 2013
Available online 26 November 2013

Communicated by: Associate Editor Gion Calzaferri

Abstract

Ag core–TiO_2 shell (Ag@TiO_2) structured nanoparticles with Ag to TiO_2 molar ratio of 1:1.7 were synthesized using one pot synthesis method and post calcination was carried out at 450 °C for 3 h to convert it from amorphous to crystalline form. The Ag core and TiO_2 shell formation was confirmed by TEM and AFM. The particle size analysis revealed the average size of Ag@TiO_2 as approximately around 30 nm. EDS spectra showed the presence of O, Ag, and Ti elements. The improvement in optical properties was proved by DRS which showed significant red shift by Ag core in visible region. Ag@TiO_2 exhibited better photocatalytic activity as compared to Degussa P25-TiO_2, synthesized TiO_2, and the Ag doped TiO_2 photocatalysts under UV and solar light irradiation for degradation of Reactive Blue 220 (RB-220) dye. Higher rate of photocatalysis of RB-220 with Ag@TiO_2 was obtained under solar light irradiation as compared to UV light irradiation, confirming the capability of the catalyst to absorb both UV and visible light. The kinetics of degradation of dye was found to follow modified Langmuir Hinshelwood (L–H) kinetic model. Ag@TiO_2 can be recycled without much decline in the efficacy. Ag@TiO_2 has been found to be the effective photocatalyst for degradation of water contaminated with azo dyes under both UV and solar light irradiations.

Keywords: Ag@TiO_2 core–shell nanoparticles; Photocatalysis; UV light; Solar light irradiation

1. Introduction

Among all the industrial sectors, textile wastewater is considered as the most polluting and the main concerns involve the adverse effects of azo dyes in the environment. Because of non biodegradable nature of textile wastewater, conventional processes are commonly ineffective for their treatment and also due to strict environmental regulations laid by many governments with reference to disposal of wastewater from the dye industries; it has become necessary to develop economically friendlier methods for the wastewater treatment (Torrades et al., 2004; Vilar et al., 2011).

Solar energy has the potential to provide for the future energy needs (Li et al., 2013) and exploitation of this alternate energy resource is the prime aim of 21st century Engineer and Scientist (Bokare et al., 2013). Solar light induced photocatalysis has attracted extensive attention due to its compliance with green chemistry concept in promoting innovative technologies (Malato et al., 2003). Solar energy can be converted into chemical energy by photocatalysts which can be used for degradation of dyes in wastewater for its treatment (Sharma et al., 2012). Among various semiconductor oxide photocatalysts, titanium dioxide (TiO_2) has gained much interest. However, it lacks in

* Corresponding author. Tel.: +91 824 2474000x3606; fax: +91 824 2474033.
E-mail addresses: ankitakhanna1987@gmail.com (A. Khanna), vidyaks68@yahoo.com (V.K. Shetty).

0038-092X/$ - see front matter © 2013 Elsevier Ltd. All rights reserved.
http://dx.doi.org/10.1016/j.solener.2013.10.032

efficiency due to high band gap and low quantum yield. It cannot be used in sunlight which consists only 4–5% of UV irradiations (Dalrymple et al., 2010). Therefore technological use of TiO_2 is largely impaired (Sakthivel and Kish, 2003). Using UV irradiation for the treatment of industrial wastewater is not only costly but also not feasible as UV light in bulk can be hazardous. In countries like India which receives huge amount of solar light for almost 10 months in a year (Singh et al., 2011), solar photocatalysis can be preferable. So, there is a need of effective photocatalysts which can be excited by both UV and Visible light of solar irradiation. While comparing organic degradation using artificial UV radiation and that by solar radiation, it has been found that the latter process demonstrates to be economically and technically feasible (Vineetha et al., 2013). Efforts have been made in recent years to enhance photocatalytic activity of TiO_2 through photocatalyst modifications such as noble metal deposition on a TiO_2 surface and shifting of the absorption spectrum of TiO_2 towards the visible-light range. Although, this type of catalyst structure is effective, it has few drawbacks that it exposes the noble metal to surroundings, making it more susceptible to corrosion (Hirakawa and Kamat, 2005). An efficient way to overcome these drawbacks is to exploit a core–shell-type structure in which the noble metal is introduced as core and the semiconductor dioxide such as TiO_2 as shell (Tom et al., 2003; Ung et al., 1998; Chan and Barteau, 2005; Pastoriza-Santos et al., 2000). Among core–shell nanoparticles, Ag@TiO_2 (Ag core and TiO_2 shell) has potentially wide applications, as TiO_2 shows properties like photoelectrochemical activity, solar energy conversion, and photocatalytic activity (Pastoriza-Santos et al., 2000; Zhou and Antonietti, 2003; Rodriguez-Gattorno et al., 2002) and also since silver nanomaterials have some unique properties of electron charge transfer and surface plasmon resonance (Hirakawa and Kamat, 2004). Hirakawa and Kamat (2005) have reported the effective separation of photogenerated electron and hole pair which may lead to enhancement of photocatalytic efficiency of Ag@TiO_2 nanoparticles. The study of core–shell metal nanoparticles has gained much attention because of these promising applications and some research groups have been focusing on the synthesis of high quality Ag@TiO_2 core–shell nanoparticles. Previous studies (Jang et al., 2006; Hara et al., 2005; Wong and Chu, 2003) have shown that the presence of shell in amorphous form hinders its usage, as most of applications require it in well crystallized form because of high photoactivity and photovoltaic properties of anatase phase of TiO_2. This problem is overcome by calcination that induces crystalline form of nanoparticles. Though Kim et al. (2004), and Zhang et al. (2005) have calcined Ag@TiO_2, there was no evidence of the retainment of the structure of Ag@TiO_2 after calcination.

In the present study, Ag@TiO_2 photocatalysts were synthesized and calcination was done to obtain TiO_2 in its crystalline form and then photocatalytic activity of these nanoparticles were examined on RB-220, an azo dye, under UV and solar light irradiation and then it was compared with other photocatalysts.

2. Experimental

2.1. Materials

Titanium (IV)-(triethanolaminato) isopropoxide solution) (TTEAIP) and Titanium (IV) tetra isopropoxide (TTIP) were purchased from Sigma–Aldrich. Reactive Blue (RB-220) was purchased from Dystar, 2-Propanol, Dimethyl Formamide (DMF), Glycine, Nitric acid, acetic acid, ethanol, and silver nitrate were purchased from the Merck. Degussa P-25 was obtained as a gift pack from Evonik Degussa India Pvt. Ltd., it consists of 25% and 75% rutile and anatase phases of TiO_2, respectively, with a specific BET (Brunauer–Emmett–Teller) surface area of 50 m^2/g, and primary particle size of 20 nm. All these chemicals were used without further purification.

2.2. Synthesis of Ag@TiO_2, TiO_2 and Ag doped TiO_2 nanoparticles

Ag@TiO_2 core–shell structured nanoparticles were prepared using one pot synthesis method of Hirakawa and Kamat (2005) with a little modification. Ag^+/TTEAIP molar ratio was optimized by prior experiments and ratio of 1:1.7 was found to be the optimum. The method for the preparation of Ag@TiO_2 nanoparticles is as follows: A mixture comprising of 15 mL of TTEAIP (8.3 mM) prepared in 2-propanol and 5 mL of $AgNO_3$ (15 mM) were stirred in a round bottom flask for 15 min at room temperature and then 10 mL of DMF was added to it. The mixture was heated to 85 °C, with a reflux and continuous stirring until the color of the mixture slowly changed from colorless to light brown and later to dark brown at the end of 90 min. At this point, the heating was stopped and the suspension was stirred till it was cooled to room temperature. The cluster suspension of Ag@TiO_2 was then centrifuged and resuspended in 5 mL of ethanol. After repeated washing with ethanol and centrifugation, to minimize the water content and DMF present in the suspension, the particles were dried in a hot air oven at 100 °C for 2 h and then calcined in a muffle furnace at 450 °C for 3 h.

For synthesis of sol–gel synthesized TiO_2 ($SGTiO_2$) and combustion synthesized TiO_2 ($CSTiO_2$), the methods given by Rupa et al. (2009) and Nagaveni et al. (2004) were followed, respectively. For the synthesis of sol–gel synthesized TiO_2 with doped silver (Ag doped-$SGTiO_2$), method reported by Zhang et al. (2008) and for combustion synthesized TiO_2 with Ag doping by liquid impregnation (Ag doped (LI)-$CSTiO_2$), method reported by Sahoo et al. (2005) and Behnajady et al. (2008) and for combustion synthesized TiO_2 with Ag doping by photodeposition (Ag doped (PD)-$CSTiO_2$), method given by Behnajady et al.

(2008) were followed. Ag to TiO_2 molar ratio of 1:1.7 was used for the synthesis of Ag doped TiO_2 catalysts.

2.3. Characterization of Ag@TiO_2 photocatalysts

The X-ray diffraction (XRD) was done for the calcined Ag@TiO_2 photocatalyst using JEOL X-ray Diffractometer with CuK-alpha radiation. The average crystallite size was obtained using the Scherrer's equation (Khanna and Shetty, 2013). The transmission electron microscopy (TEM), and energy dispersive spectra (EDS was performed using a JEOL-JEM-2100 F microscope operating at an acceleration potential of 200 kV as explained by Khanna and Shetty (2013). Atomic Force Microscopy (AFM) measurements and imaging were carried out using a scanning probe microscope (NT-MDT, NTEGRA). The Optical absorption characterization of the Ag@TiO_2 nanoparticles was done using diffuse reflectance spectroscopy (DRS) (Varian Cary 5000 Spectrometer).

2.4. Experimental setup for degradation of Reactive Blue-220 under UV and solar light irradiation

The experimental setup for UV photocatalysis consisted of an aluminum chamber of 40 cm × 70 cm × 70 cm dimensions equipped with two 18 W UV lamps (wavelength, $\lambda = 365$ nm, Philips), which were placed vertically, specified to radiate 80% UV-A and 20% UV-B light. UV light intensity was measured using a UV light meter (UV-340A, Lutron) and an average light intensity at the reactor wall was found to be 5.85 mW/cm^2. An exhaust fan was fitted on top of the chamber to drive out heated air and to maintain a constant temperature inside the reactor. A 250 mL capacity borosilicate glass beaker was used as the reactor and it was placed equidistant from both the UV lamps. Same reactor was used for solar experiments and experiments were done in an open terrace. Solar experiments were conducted in the month of November between 11 am to 12 noon and an average UV and visible light intensity (KM-LUX-100K) were found to be 3.62 mW/cm^2, and 1120 × 10^2 lux respectively. The reaction mixture was magnetically stirred.

2.5. Experimentation

Batch experiments for the photocatalytic degradation of RB-220 were conducted using the synthesized Ag@TiO_2 core–shell structured photocatalysts and different TiO_2 and Ag doped TiO_2 photocatalysts (SGTiO_2, CSTiO_2, Ag doped-SGTiO_2, Ag doped (LI)-CSTiO_2, and Ag doped (PD)-CSTiO_2) under UV and Solar light irradiation. The synthetic dye solution (100 mL) was prepared with a dye concentration of 50 mg/L and the pH was adjusted to 3 using 0.01 N H_2SO_4 solution. 1 g/L of photocatalyst was added to the synthetic dye solution and the reactor containing this solution was placed inside the experimental chamber under constant stirring with a magnetic stirrer. Air as the oxidant was bubbled through the reactor at a flow rate of 2 LPM for UV photocatalysis. No additional air supply was provided for experiments under solar light as, for experimental duration of one hour, the results obtained with and without the supply of air were similar, owing to dissolved oxygen being present in aqueous dye solution. 3 mL of sample was withdrawn from the reaction mixture at regular time intervals for the analysis of dye concentration and centrifuged at 10,000 RPM for 5 min to separate the catalyst prior to analysis. The absorbance of the solution at 609 nm (the wavelength which showed maximum absorption for RB-220), was measured using a UV–Vis spectrophotometer (model: U-2000, Hitachi). The dye concentration of unknown sample was calculated using the calibration plot and the absorbance. The percentage of degradation of dye was estimated using the following equation:

$$\textit{degradation}\ (\%) = (C_0 - C)/C_0 \times 100 \quad (1)$$

where C_0 and C are the concentrations of dye at initial and at a particular time in a reactor, respectively. The photocatalytic activity of different TiO_2 and Ag doped TiO_2 photocatalysts in terms of degradation of RB-220 were compared with that of Ag@TiO_2 core–shell structured photocatalysts under UV and Solar light. All the experiments under UV and solar light were carried out in triplicates, and mean values were used for analysis, at each interval of time.

3. Results and discussion

3.1. Characterization of Ag@TiO_2

X-ray diffractograms of the synthesized Ag@TiO_2 nanoparticles after post calcination has been reported elsewhere by the authors (Khanna and Shetty, 2013). Fig. 1 shows the TEM image which confirmed the formation of Ag core and TiO_2 shell. The Ag@TiO_2 nanoparticles showed Ag core with approximate dimension of 33.63 nm and TiO_2 shell

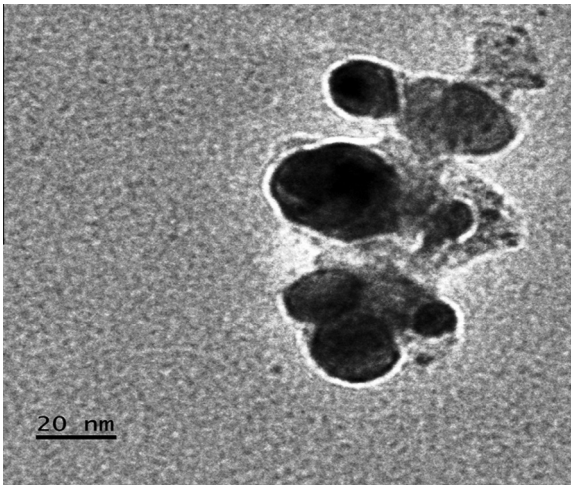

Fig. 1. TEM image of Ag@TiO_2 nanoparticles calcined at 450 °C.

of average thickness of 3.7 nm (Khanna and Shetty, 2013). The crystalline structure of both Ag core and TiO_2 shell was confirmed by X-ray diffractogram of $Ag@TiO_2$ nanoparticles calcined at 450 °C (Khanna and Shetty, 2013). No AgO reflection peak ($2\theta = 30.2$) was observed in the diffraction pattern, indicating Ag core exist as Ag^0 in $Ag@TiO_2$. Absence of AgO indicates that there is no possibility of decrease in photocatalytic activity due to the presence of AgO, as reported by Wang et al. (2008).

Fig. 2 illustrates the EDS spectra of $Ag@TiO_2$ nanoparticles. The presence of Cu in spectra was due to the copper grid used in the TEM measurement. The elemental compositions of the $Ag@TiO_2$ photocatalysts obtained from the EDS analysis showed the presence of O, Ti, and Ag elements.

The AFM image (Fig. 3) reveals the formation of $Ag@TiO_2$ nanoparticles. As it can be seen in Fig. 3, silver is in the form of well-defined oval nanoparticles which is covered by TiO_2 shell. This analysis is in good agreement with the TEM analysis. These analyses confirmed the retainment of core–shell structure even after calcination. Fig. 4 presents the particle size distribution curve of $Ag@TiO_2$ nanoparticles which shows that the nanoparticles are polydispersed and the size varied in the range of 10–50 nm with the average particles size of approximately 30 nm. This result is in good agreement with XRD and TEM results (Khanna and Shetty, 2013). The double peaks corresponding to particles of size 26 and 32 nm in the size distribution curve indicate that these two particles sizes are found more frequently in the distribution.

The DRS of the $Ag@TiO_2$ nanoparticles (Fig. 5) showed a sharp reflectance peak at 320 nm in the UV region which is the characteristic of TiO_2 corresponding to the charge transfer process from the valence band to conduction band in TiO_2 (Li et al., 2008). The $Ag@TiO_2$ also shows strong visible light absorption in the range of 398–509 nm and maximum is seen at 509 nm. So $Ag@TiO_2$ is able to absorb both UV light and portion of visible light, maximum visible light absorption being at 509 nm. The visible light absorption of $Ag@TiO_2$ particles, as seen by the occurrence of red shift is due to the surface plasmon resonance of Ag core and it is strongly influenced by the oxide shell (Rodriguez-Gattorno et al., 2002). The high dielectric constant of the TiO_2 shell causes a red shift in the plasmon absorption of the silver core (Chan and Barteau, 2005; Mulvaney, 1996; Liz-Marzán and Mulvaney, 2003; Kreibig and Vollmer, 1995). The ability of these core–shell nanoparticles to absorb both UV and visible light shall enhance their photocatalytic activity in solar light, which constitutes small portion of UV and majority being the visible light.

3.2. Comparison of photocatalytic activity of $Ag@TiO_2$ core shell structured nanoparticles with other photocatalysts under UV and Solar light irradiation

The efficacy of $Ag@TiO_2$ nanoparticles as a photocatalyst was compared with other catalysts such as TiO_2 and Ag doped TiO_2 based on the degradation of RB-220 under UV and solar light irradiations. So, the efficiency of $Ag@TiO_2$ for degradation RB-220 dye with initial concentration of 50 mg/L, and at pH 3 was compared with commercially available Degussa P-25 catalyst, $SGTiO_2$, $CSTiO_2$, Ag doped-$SGTiO_2$, Ag doped(LI)-$CSTiO_2$, and Ag doped (PD)-$CSTiO_2$. In all the experiments, catalyst loading of 1 g/L for UV photocatalysis and 500 mg/L for solar photocatalysis was used. In case of UV light air was bubbled through the solution continuously to act as an oxidant. In case of solar light, continuous bubbling of air was not necessary as the results obtained in the presence and absence of air bubbling matched with each other, indicating that dissolved oxygen (DO) present in the reaction mixture initially and subsequent dissolution from atmospheric air during the experiments itself was sufficient to serve as an oxidant, for the reaction duration of one hour. The photocatalytic degradation of RB-220 by different catalysts at various irradiation times are shown in Fig. 6(a and b) for UV and solar light irradiations respectively. These figures clearly show that $Ag@TiO_2$ nanoparticles are more efficient in degradation of the RB-220 dye as compared to other catalysts and photocatalytic activity is in the order of

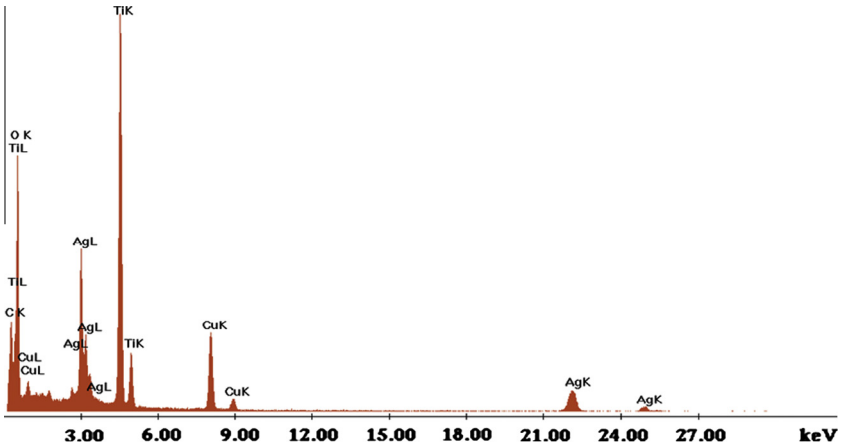

Fig. 2. EDS spectra of $Ag@TiO_2$ nanoparticles calcined at 450 °C.

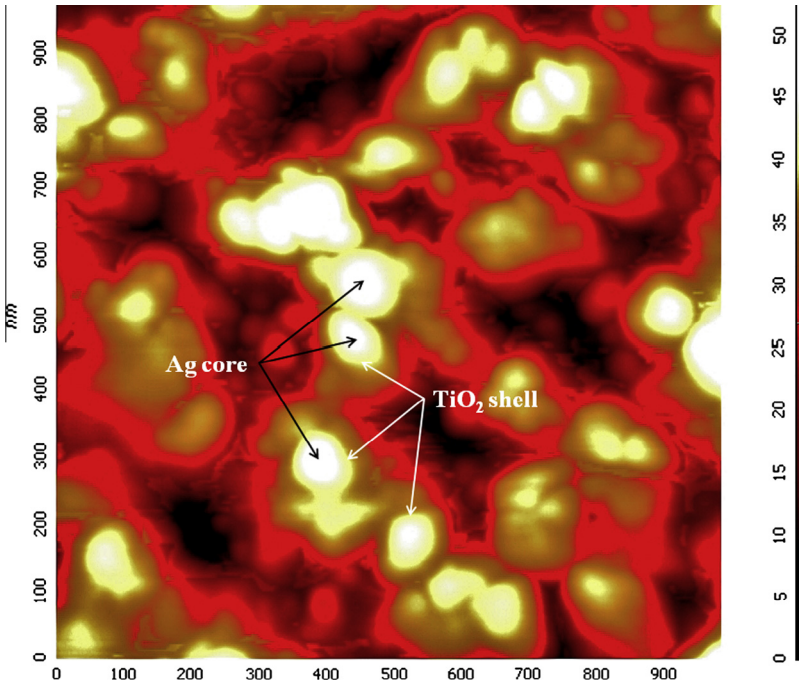

Fig. 3. AFM image of $Ag@TiO_2$ nanoparticles calcined at 450 °C.

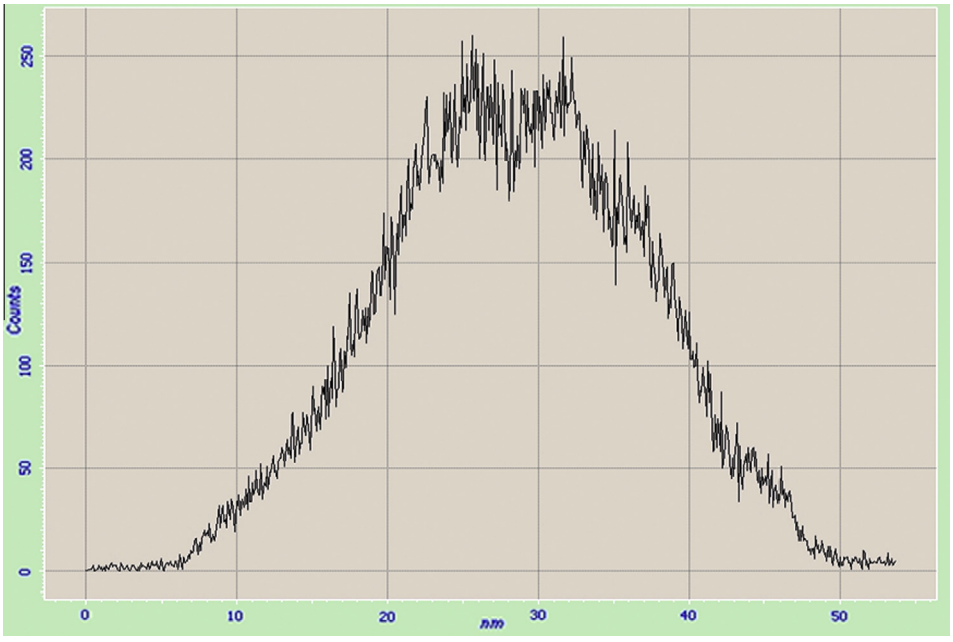

Fig. 4. Particle size distribution of $Ag@TiO_2$ nanoparticles calcined at 450 °C.

$Ag@TiO_2$ > Degussa P25 > Ag doped-$SGTiO_2$ > $SGTiO_2$ > $CSTiO_2$ > Ag doped (PD)-$CSTiO_2$ > Ag doped (LI)-$CSTiO_2$ under UV light and under solar irradiation the activity is rated as $Ag@TiO_2$ > Ag doped-$SGTiO_2$ > Degussa P25 > $SGTiO_2$ > $CSTiO_2$ > Ag doped (PD)-$CSTiO_2$ > Ag doped (LI)-$CSTiO_2$. High photocatalytic efficiency is exhibited by $Ag@TiO_2$ under UV and solar light which might be due to their ability to inhibit electron–hole recombination, by storage of electron in Ag core and subsequent discharge on provision of electron acceptor such as O_2 (Hirakawa and Kamat, 2005) and also owing to their capability to absorb both UV and visible light radiations of solar light. In case of solar light with $Ag@TiO_2$ catalyst, almost 100% degradation of RB-220 occurred within 60 min, whereas with UV light, it took around 240 min. It was found that catalyst loading and time required for solar photocatalysis is much lesser than that used in UV photocatalysis. Also compared to UV, under solar light

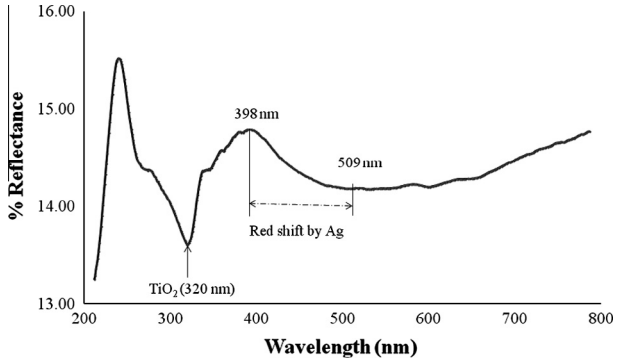

Fig. 5. DRS spectrum of Ag@TiO_2 nanoparticles calcined at 450 °C.

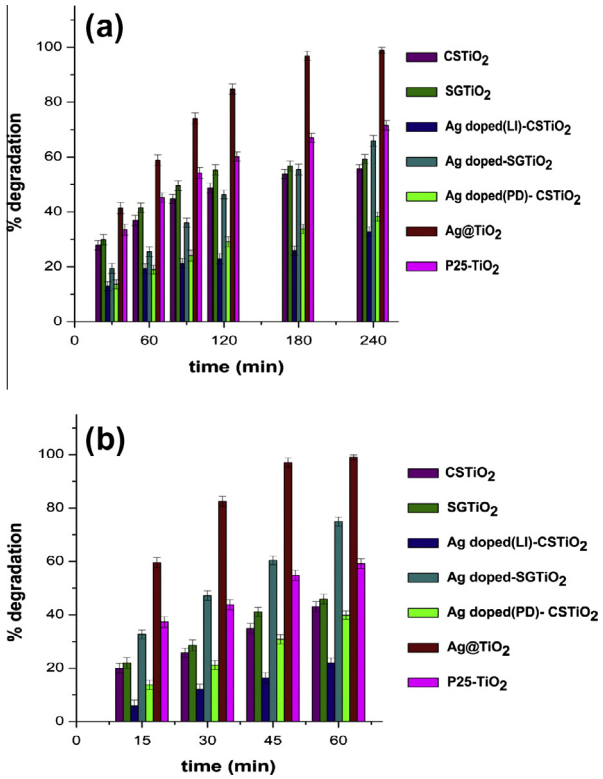

Fig. 6. Comparison of photocatalytic activity of different photocatalysts in terms of degradation of RB-220 dye: initial pH = 3, and initial concentration = 50 mg/L (a) UV light (Catalyst loading = 1 g/L) (b) solar light (Catalyst loading = 500 mg/L). The Error bars correspond to the 95% confidence limit.

rate of photocatalysis was very high with Ag@TiO_2 catalyst, due to its potential to absorb both UV and visible light portions of solar radiation, as indicated by DRS spectrum shown in Fig. 5.

Lower photocatalytic efficacy exhibited by Degussa P25, $SGTiO_2$, and $CSTiO_2$ may be due to the electron–hole recombination, leading to low quantum yield. However, less photocatalytic efficacy exhibited by Ag doped-$SGTiO_2$ and Ag doped (LI)-$CSTiO_2$, may be due to the loss of activity of TiO_2, as metal deposits occupy the active sites on the TiO_2 surface (Coleman et al., 2005). Also less activity was shown by Ag doped (PD)-$CSTiO_2$ as the negative charge on silver may start to attract holes and then recombine with electrons leading to recombination of electron–hole (Carp et al., 2004) thus lowering the photocatalytic activity.

As shown in Fig. 7, the Ag@TiO_2 reduces the electron–hole recombination by storing electron in Ag core, so electron and holes becomes free charge carriers in the conduction and valance bands and thus retard the electron–hole recombination. The electron will get discharged when an electron acceptor such as oxygen is supplied (Hirakawa and Kamat, 2005). We propose a possible mechanism of photocatalytic activity of Ag@TiO_2 for the photocatalytic degradation of RB-220, on the similar basis as explained by Abdulla-Al-Mamun et al. (2011) on the mechanism of the Ag@TiO_2 photocatalytic activity against cancer cells. As shown in Fig. 7 (Eqs. (1) and (2)), the photo excited electrons are penetrated or transferred quickly through TiO_2 shell into the Ag nanocore until the Fermi level charge equilibrium is attained between the shell and core systems, after which the electrons are facilitated to quickly transfer from excited TiO_2, initiating the redox reactions at the interface of TiO_2 shell and dye solution (Abdulla-Al-Mamun et al., 2010). Further electrons can easily react with O_2 and form active species H_2O_2, $O_2^{\cdot-}$, $HO_2^{\cdot}$ (Sung-Suh et al., 2004) which considerably advance the photocatalytic degradation of RB-220. These active species further react and produce hydroxyl radical ($^{\cdot}OH$). In addition, it was reported that holes will react with adsorbed water molecules, leading to the production of $^{\cdot}OH$ as shown in Eqs. (3) and (4) (Jaeger and Bard, 1979; Cai et al., 1992). On the photoexcitation of Ag@TiO_2, reactive oxygen species such as hydroxyl radicals and hydrogen peroxide are formed which are highly oxidizable species and expected to be responsible for the photocatalytic degradation of RB-220 (Abdulla-Al-Mamun et al., 2010). The electron storage and discharge will take place until equilibrium is attained (Hirakawa and Kamat, 2005). The storage of electron in Ag core decreases the electron density within the TiO_2 and leads to an increase in the hydroxyl group acidity which in turn affects the photocatalytic degradation (Rhoderick and Williams, 1988; Jafiezic-Renault et al., 1986). The Ag metal also has unique property of charge transfer and visible light absorption which leads to enhanced photocatalytic degradation of RB-220 than TiO_2 and Ag doped TiO_2.

Hence it may be concluded that Ag@TiO_2 nanoparticles are responsive to even visible light and hence are the efficient catalysts for the photocatalytic degradation of dyes under UV and solar light irradiation.

3.3. Photocatalytic degradation of RB-220 dye

In order to confirm that the degradation of RB-220 is due to photocatalysis, the photodegradation of RB-220 was studied (a) under a light source (UV and solar) and in the absence of any catalyst, (b) under dark conditions

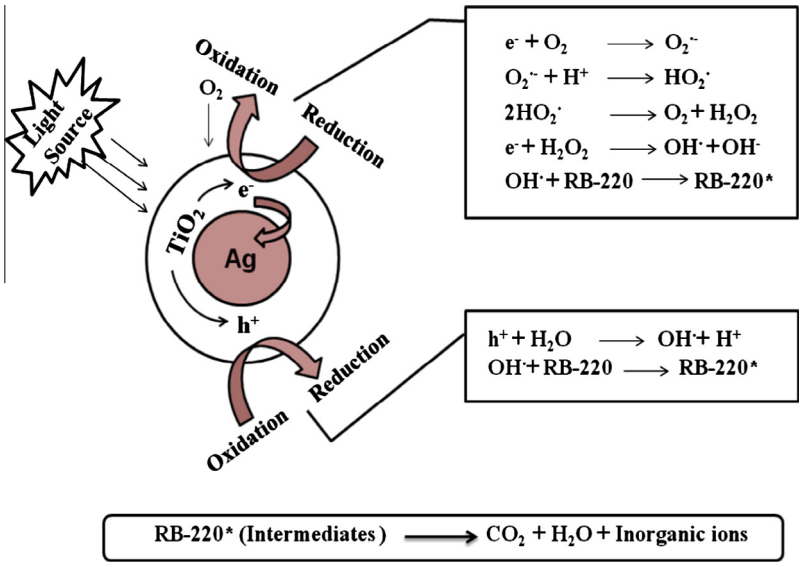

Fig. 7. Proposed Mechanism of Photocatalytic degradation of RB-220 using calcined Ag@TiO_2 nanoparticles.

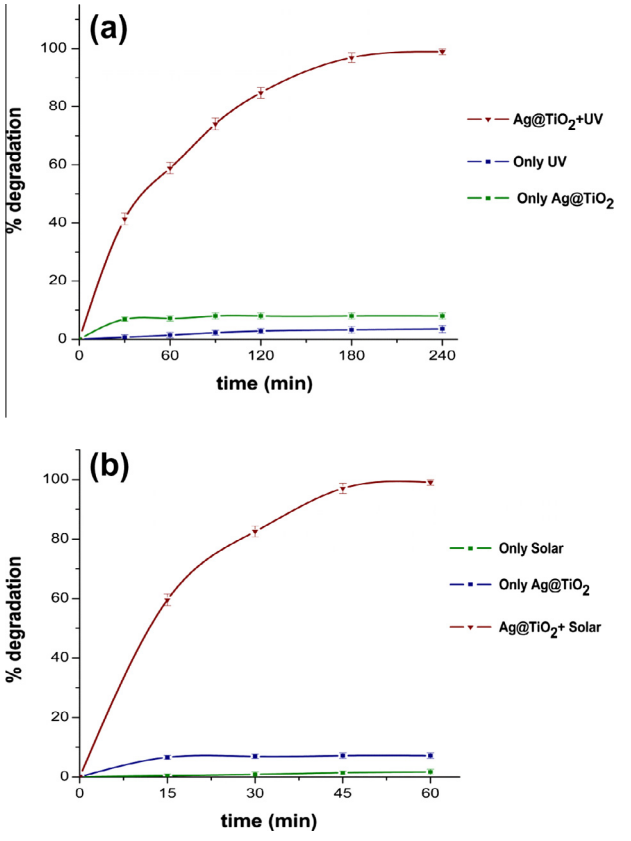

Fig. 8. Photocatalytic degradation of RB-220 dye: initial pH = 3, and initial concentration = 50 mg/L (a) UV light (Catalyst loading = 1 g/L) (b) solar light (Catalyst loading = 500 mg/L). The Error bars correspond to the 95% confidence limit.

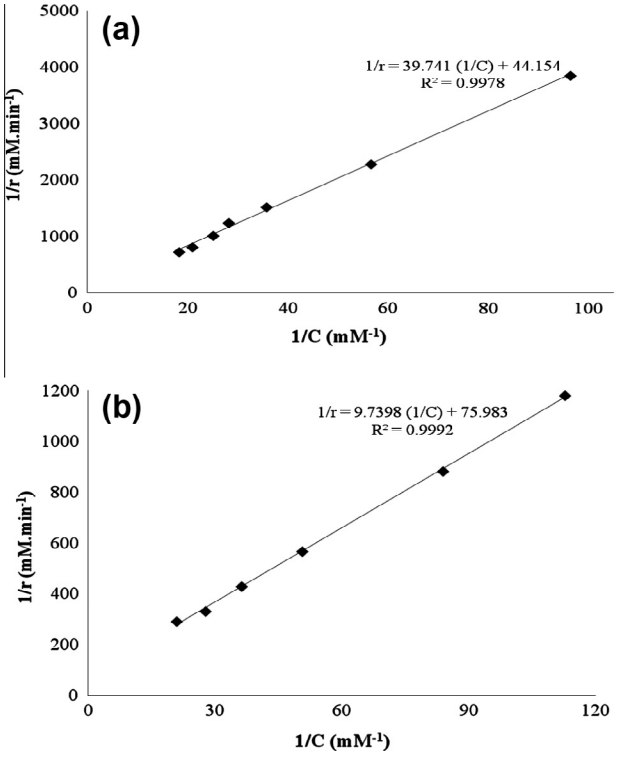

Fig. 9. Plot for L–H kinetics of degradation of RB-220 dye using Ag@TiO_2 as catalyst at conditions: pH = 3 (a) UV light (catalyst used = 1 g/L) (b) solar light (catalyst used = 500 mg/L).

with Ag@TiO_2 nanoparticles, and (c) with Ag@TiO_2 under UV and solar light irradiations. Fig. 8(a and b) shows the comparison of degradation of RB-220 as the function of time for control experiments (either light or Ag@TiO_2) along with the results obtained when UV and solar light was used with Ag@TiO_2. The initial concentration of RB-220 used was 50 mg/L. No significant dye degradation occurred in the absence of catalyst and RB-220 solution was found to be stable on irradiation with UV and solar light irradiation, indicating that no photolysis occurs. Under dark conditions and in the presence Ag@TiO_2, around 7% degradation of RB-220 dye occurred in 60 min and around 8% degradation occurred after

240 min of irradiation. This is due to the adsorption of dye molecule on the surface of Ag@TiO_2. On the other hand degradation of dye increased drastically and almost complete degradation of dye occurred within 240 min under UV irradiation and within 60 min under solar light irradiation when Ag@TiO_2 at loading of 1 g/L was used as catalyst. The rate of degradation of RB-220 with catalyst under solar light was tremendously faster as compared to that with catalyst under UV light. As explained in Section 3.2, illumination of Ag@TiO_2 leads to formation of reactive species such as H_2O_2, $O_2^{\cdot-}$ and $^{\cdot}OH$ which attack the azo bond of RB-220 and this lead to cleavage of azo bond and caused decolorization of dye solution. This clearly shows that the phenomenon of degradation of RB-220 dye is photocatalysis by Ag@TiO_2 nanoparticles under UV and solar light irradiation.

Study on kinetics of degradation of the dye is important with reference to design of photocatalytic reactors for treatment of dye wastewater. Rate equation determination and estimation of the parameters of the rate equation are important part of kinetics. So, kinetics of degradation of RB-220 was studied under UV and solar light irradiations at initial dye concentration of 50 mg/L, and pH of 3. In case of UV light, catalyst loading of 1 g/L and in case of solar 500 mg/L of Ag@TiO_2 was used. To evaluate the heterogeneous photocatalytic reaction successfully, the modified Langmuir–Hinshelwood (L–H) kinetic expression have been used by numerous researchers (Chen and Ray, 1998; Galindo et al., 2001; Muruganandham and Swaminathan, 2004; Wenhua et al., 2000). The data obtained by conducting the photocatalysis experiments has been rationalized in terms of the modified form of L–H kinetic model. The effect of dye concentration on the rate of degradation is given in the form of (Eq. (2)) (Matthews, 1987)

$$r = \frac{k_1 k_2 [C]}{(1 + k_2 [C])} \tag{2}$$

where (r) is the reaction rate of RB-220 dye, C is the concentration of the dye at time 't', k_1 the constant related to adsorption and k_2 is the reaction rate constant.

$$\frac{1}{r} = \frac{1}{k_1 k_2 [C]} + \frac{1}{k_1} \tag{3}$$

To estimate the parameters in Eq. (3), rates of degradation were obtained by drawing tangents at different interval of time, on plots of dye concentration versus time data obtained from the experiment. $1/(r)$ versus $1/C$ is plotted and values for the kinetic parameters are estimated from the slope and intercept. The applicability of L–H equation has been confirmed by the linear nature of the plot as shown in Fig. 9. This indicates that the degradation of dye occurred mainly on the surface of Ag@TiO_2. The values of k_1 and k_2 for degradation of RB-220 under UV and solar light irradiation are presented in Table 1. The rate of degradation of RB-220 dye by the surface reaction is proportional to the surface coverage of dye on the Ag@TiO_2 assuming that the dye is strongly adsorbed on the catalyst surface than the intermediate products (Al-Ekabi and Serpone, 1988).

3.4. Effect of recycling of Ag@TiO_2

In order to prove the efficacy of reused Ag@TiO_2 nanoparticles, experiments were carried out with similar reaction conditions under UV and solar light irradiations. After completion of experiment with a fresh catalyst (cycle I), the Ag@TiO_2 nanoparticles at the end of cycle I was collected and then utilized for the next set of recycle experiments. Ag@TiO_2 was reused thrice and totally four experiments were done, out of which the first cycle was with the fresh catalyst and the remaining three cycles were with the recycled catalyst. Before next cycle of experiment, the catalyst was centrifuged at 10,000 rpm for 10 min to separate it from the treated water. It is then washed thrice with ethanol. In order to remove ethanol from the wet particles after centrifugation, particles were dried in an oven at 100 °C for 2 h. Then next cycle of batch experiments were conducted and same experimental conditions were used for all the four cycles. The% degradation of dye using fresh particles (Cycle I), particles of single prior use (Cycle II), particles of two prior uses (Cycle III), and particles of three prior uses (Cycle IV) after 240 min of irradiation for UV and 60 min for Solar are given in Table 2. After three cycles of reuse, decrease in photocatalytic activity from around 98.92% to 96.36% was observed under UV light irradiation (240 min) and from 99.02% to 97.14% under solar light

Table 1
Values of $k_1$and k_2 for percentage degradation of RB-220 under UV and solar light irradiation.

UV light		Solar light	
k_1 (mM min^{-1})	k_2 (mM)$^{-1}$	k_1 (mM min^{-1})	k_2 (mM)$^{-1}$
0.023	1.11	0.013	7.80

Table 2
Effect of catalyst recycling on percentage degradation of RB-220 dye under.

Cycle number	% Degradation of RB-220 after 240 min
(a) UV light irradiation (The degradation following plus and minus sign corresponds to 95% confidence limit)	
Fresh (I)	98.92 ± 1.02
II	98.09 ± 1.14
III	97.11 ± 1.25
IV	96.36 ± 1.18
	% Degradation of RB-220 after 60 min
(b) Solar light irradiation (The degradation following plus and minus sign corresponds to 95% confidence limit)	
Fresh (I)	99.02 ± 0.93
II	98.47 ± 1.08
III	98.02 ± 1.13
IV	97.14 ± 1.28

irradiation (60 min). The reduction in activity was found to be only less than 4% after three cycles of reuse. So it can be concluded that Ag@TiO_2 can be recycled without much decline in activity and the recycled catalyst can be reused for the photocatalysis of dyes using UV and solar irradiation.

4. Conclusions

The Ag@TiO_2 core–shell structured nanoparticles were synthesized by one pot synthesis route, calcined at 450 °C and were used as photocatalyst for the photocatalytic degradation of RB-220 dye under UV and solar light. TEM and AFM confirmed the retainment of core shell structure of Ag@TiO_2 after calcination at 450 °C. The EDS spectrum shows the presence of O, Ti and Ag elements. The particle size distribution shows that the size of nanoparticles varies from 10 to 50 nm with an average size of 30 nm. DRS indicated that Ag@TiO_2 is able to absorb both UV light and visible light, maximum visible light absorption being at 509 nm. Photocatalytic activity of Ag@TiO_2 nanoparticles in terms of degradation of RB-220 was compared with that of other TiO_2 and Ag doped TiO_2 photocatalysts and Ag@TiO_2 was proved to be highly efficient catalyst in both UV as well as solar irradiation as compared to other catalysts. Solar photocatalysis has been shown to be more efficient than UV photocatalysis, with Ag@TiO_2 nanoparticles. Enhanced rate of degradation of RB-220 was obtained under solar light irradiation as compared to UV light irradiation and thus solar photocatalysis using Ag@TiO_2 nanoparticles can serve as an alternative technology for dye degradation owing to low power requirements and higher efficiency. The kinetics of degradation of RB-220 dye followed modified Langmuir Hinshelwood (L–H) kinetic model. Ag@TiO_2 can be reused at least thrice without much decline in photocatalytic efficiency. Hence photocatalytic degradation of RB-220 dye using Ag@TiO_2 core–shell structured nanoparticles can be exploited for the treatment of dye/textile wastewater under UV and solar light irradiation. Solar photocatalysis using Ag@TiO_2 can prove to be an energy efficient and cost effective method.

Acknowledgement

Authors thank the Department of Science and Technology, Government of India for providing the financial support to carry out this research work.

References

Abdulla-Al-Mamun, M., Kusumoto, Y., Ahmmad, B., Islam, M.S., 2010. Photocatalytic cancer (HeLa) cell-killing enhanced with Cu–TiO_2 nanocomposite. Top. Catal. 53, 571–577.

Abdulla-Al-Mamun, M., Kusumoto, Y., Ahmmad, B., Islam, M.S., 2011. Synergistic cell-killing by photocatalytic and plasmonic photothermal effects of Ag@TiO_2 core–shell composite nanoclusters against human epithelial carcinoma (HeLa) cells. Appl. Catal. A 398, 134–142.

Al-Ekabi, H., Serpone, N., 1988. Kinetic studies in heterogeneous photocatalysis. 1. Photocatalytic degradation of chlorinated phenols in aerated aqueous solution over TiO_2 supported on a glass matrix. J. Phys. Chem. 92, 5726–5731.

Behnajady, M.A., Modirshahla, N., Shokri, M., Rad, B., 2008. Enhancement of photocatalytic activity of TiO_2 nanoparticles by silver doping: photodeposition versus liquid impregnation methods. Global NEST J. 10, 1–7.

Bokare, A., Pai, M., Athawale, A.A., 2013. Surface modified Nd doped TiO_2 nanoparticles as photocatalysts in UV and solar light irradiation. Sol. Energy 91, 111–119.

Cai, R., Kubota, Y., Shuin, T., Sakai, H., Hashimoto, K., Fujishima, A., 1992. Increment of photocatalytic killing of cancer cells using TiO_2 with the aid of superoxide dismutase. Chem. Lett. 3, 427–430.

Carp, O., Huisman, C.L., Reller, A., 2004. Photoinduced reactivity of titanium dioxide. Prog. Solid State Chem. 33, 33–177.

Chan, S.C., Barteau, M.A., 2005. Preparation of highly uniform Ag/TiO_2 and Au/TiO_2 supported nanoparticle catalysts by photodeposition. Langmuir 21, 5588–5595.

Chen, D., Ray, A.K., 1998. Photodegradation kinetics of 4-nitrophenol in TiO_2 suspension. Water Res. 32, 3223–3234.

Coleman, H.M., Chiang, K., Amal, R., 2005. Effects of Ag and Pt on photocatalytic degradation of endocrine disrupting chemicals in water. Chem. Eng. J. 113, 65–72.

Dalrymple, O.K., Stefanakos, E., Trotz, M.A., Goswami, D.Y., 2010. A review of the mechanisms and modeling of photocatalytic disinfection. Appl. Catal. B 98, 27–38.

Galindo, C., Jacques, P., Kalt, A., 2001. Photooxidation of the phenylazonaphthol AO20 on TiO_2: kinetic and mechanistic investigations. Chemosphere 45, 997–1005.

Hara, K., Miyamoto, K., Abe, Y., Yanagida, M., 2005. Electron transport in coumarin-dye-sensitized nanocrystalline TiO_2 electrodes. J. Phys. Chem. B 109, 23776–23778.

Hirakawa, T., Kamat, P.V., 2004. Photoinduced electron storage and surface plasmon modulation in Ag@TiO_2 clusters. Langmuir 20, 5645–5647.

Hirakawa, T., Kamat, P.V., 2005. Charge separation and catalytic activity of Ag@TiO_2 core–shell composite clusters under UV-irradiation. J. Am. Chem. Soc. 127, 3928–3934.

Jaeger, C.D., Bard, A.J., 1979. Spin trapping and electron spin resonance detection of radical intermediates in the photodecomposition of water at TiO_2 paniculate systems. J. Phys. Chem. 93, 3146–3152.

Jafiezic-Renault, N., Pichat, P., Foissy, A., Mercier, R., 1986. Effect of deposited pt particles on the surface charge of TiO_2 aqueous suspensions by potentiometry, electrophoresis and labeled ion adsorption. J. Phys. Chem. 90, 2733–2738.

Jang, S.R., Vittal, R., Lee, J., Jeong, N., Kim, K.J., 2006. Linkage of N3 dye to N3 dye on nanocrystalline TiO_2 through trans-1, 2-bis (4-pyridyl) ethylene for enhancement of photocurrent of dye-sensitized solar cells. Chem. Commun. 1, 103–105.

Khanna, A., Shetty, V.K., 2013. Solar photocatalysis for treatment of Acid Yellow-17 (AY-17) dye contaminated water using Ag@TiO_2 core–shell structured nanoparticles. Environ. Sci. Pollut. Res. 20, 5692–5707.

Kim, Y.H., Kang, Y.S., Jo, B.G., 2004. Preparation and characterization of Ag-TiO_2 core–shell type nanoparticles. J. Ind. Eng. Chem. 10, 739–744.

Kreibig, U., Vollmer, M., 1995. In: Optical Properties of Metal Clusters, vol. 24. Springer Series in Materials Science, Berlin.

Li, H., Duan, X., Liu, G., Liu, X., 2008. Photochemical synthesis and characterization of Ag/TiO_2 nanotube composites. J. Mater. Sci. 43, 1669–1676.

Li, C., Goswami, Y., Stefanakos, E., 2013. Solar assisted sea water desalination: a review. Renew. Sust. Energy Rev. 19, 136–163.

Liz-Marzán, L.M., Mulvaney, P., 2003. The assembly of coated nanocrystals. J. Phys. Chem. B 107, 7312–7326.
Malato, S., Blanco, J., Vidal, A., Alarcón, D., Maldonado, M.I., Cáceres, J., Gernjak, W., 2003. Applied studies in solar photocatalytic detoxification: an overview. Sol. Energy 75, 329–336.
Matthews, R.W., 1987. Photooxidation of organic impurities in water using thin films of titanium dioxide. J. Phys. Chem. 91, 3328–3333.
Mulvaney, P., 1996. Surface plasmon spectroscopy of nanosized metal particles. Langmuir 12, 788–800.
Muruganandham, M., Swaminathan, M., 2004. Solar photocatalytic degradation of a reactive azo dye in TiO_2-suspension. Sol. Energy Mater. Sol. Cells 81, 439–457.
Nagaveni, K., Sivalingam, G., Hedge, M.S., Madras, G., 2004. Solar photocatalytic degradation of dyes: high activity of combustion synthesized nano TiO_2. Appl. Catal. B Environ. 48, 83–93.
Pastoriza-Santos, I., Koktysh, D.S., Mamedov, A.A., Giersig, M., Kotov, N.A., Liz-Marzán, L.M., 2000. One-pot synthesis of Ag@TiO_2 core–shell nanoparticles and their layer-by-layer assembly. Langmuir 16, 2731–2735.
Rhoderick, E.H., Williams, R.H., 1988. Metal–Semiconductor Contacts, second ed. Oxford University Press, New York.
Rodriguez-Gattorno, G., Diaz, D., Rendon, L., Hernandez-Segura, G.O., 2002. Metallic nanoparticles from spontaneous reduction of silver (I) in DMSO. Interaction between nitric oxide and silver nanoparticles. J. Phys. Chem. B 106, 2482–2487.
Rupa, A.V., Divakar, D., Sivakumar, T., 2009. Titania and noble metals deposited titania catalysts in the photodegradation of Tartrazine. Catal. Lett. 132, 259–267.
Sahoo, C., Gupta, A.K., Pal, A., 2005. Photocatalytic degradation of Crystal Violet (C.I. Basic Violet 3) on silver ion doped TiO_2. Dyes Pigments 66, 189–196.
Sakthivel, S., Kish, H., 2003. Photocatalytic and photo electrochemical properties of nitrogen-doped titanium dioxide. Chem. Phys. Chem. 4, 487–490.
Sharma, M., Jain, T., Singh, S., Pandey, O.P., 2012. Photocatalytic degradation of organic dyes under UV–Visible light using capped ZnS nanoparticles. Sol. Energy 86, 626–633.
Singh, C., Chaudhary, R., Thakur, R.S., 2011. Performance of advanced photocatalytic detoxification of municipal wastewater under solar radiation – a mini review. Int. J. Energy Environ. 2, 337–350.
Sung-Suh, H.M., Choi, J.R., Hah, H.J., Koo, S.M., 2004. Comparison of Ag deposition effects on the photocatalytic activity of nanoparticulate TiO_2 under visible and UV light irradiation. J. Photochem. Photobiol., A 163, 37–44.
Tom, R.T., Nair, A.S., Singh, N., Aslam, M., Nagendra, C.L., Philip, R., Vijayamohanan, K., Pradeep, T., 2003. Freely dispersible Au@TiO_2, Au@ZrO_2, Ag@TiO_2, and Ag@ZrO_2 core–shell nanoparticles: one-step synthesis, characterization, spectroscopy, and optical limiting properties. Langmuir 19, 3439–3445.
Torrades, F., García-Montaño, J., Antonio García-Hortal, J., Doménech, X., Doménech, J., 2004. Decolorization and mineralization of commercial reactive dyes under solar light assisted photo-Fenton conditions. Sol. Energy 77, 573–581.
Ung, T., Liz-Marzán, L.M., Mulvaney, P., 1998. Controlled method for silica coating of Silver colloids. Influence of coating on the rate of chemical reactions. Langmuir 14, 3740–3748.
Vilar, V.J.P., Pinho, L.X., Pintor, A.M.A., Rui, A.R., Boaventura, R.A.R., 2011. Treatment of textile wastewaters by solar-driven advanced oxidation processes. Sol. Energy 85, 1927–1934.
Vineetha, M.N., Matheswaran, M., Sheeba, K.N., 2013. Photocatalytic colour and COD removal in the distillery effluent by solar radiation. Sol. Energy 91, 368–373.
Wang, W., Zhang, J., Chen, F., He, D., Anpo, M., 2008. Preparation and photocatalytic properties of Fe^{3+}-doped Ag@TiO_2 core–shell nanoparticles. J. Colloid Interface Sci. 323, 182–186.
Wenhua, L., Hong, L., Suoan, C., Jianqing, Z., Chunan, C., 2000. Kinetics of photocatalytic degradation of aniline in water over TiO_2 supported on porous nickel. J. Photochem. Photobiol. A Chem. 131, 125–132.
Wong, C.C., Chu, W., 2003. The hydrogen peroxide-assisted photocatalytic degradation of alachlor in TiO_2 suspensions. Environ. Sci. Technol. 37, 2310–2316.
Zhang, D., Song, X., Zhang, R., Zhang, M., Liu, F., 2005. Preparation and characterization of Ag@TiO_2 core–shell nanoparticles in water-in-oil emulsions. Eur. J. Inorg. Chem. 2005, 1643–1648.
Zhang, L.C., Cai, K.F., Yao, X., 2008. Preparation, characterization and photocatalytic performance of Co/Ni Co-doped TiO_2 nanopowders. J. Electroceram. 21, 512–515.
Zhou, Y., Antonietti, M., 2003. Synthesis of very small TiO_2 nanocrystals in a room-temperature ionic liquid and their self-assembly toward mesoporous spherical aggregates. J. Am. Chem. Soc. 125, 14960–14961.